fluids

MDPI

Article

Influence of Body Heat Loss on Temperature and Velocity Fields in a Whole-Body Cryotherapy Chamber

Rim Elfahem [1], Bastien Bouchet [2,3], Boussad Abbes [1], Guillaume Polidori [1,*] and Fabien Beaumont [1]

[1] Laboratory of Materials Thermal and Mechanical Engineering MATIM, University of Reims Champagne Ardenne, CEDEX 2, 51687 Reims, France; rim.elfahem@etudiant.univ-reims.fr (R.E.); boussad.abbes@univ-reims.fr (B.A.); fabien.beaumont@univ-reims.fr (F.B.)
[2] Cryotera, 51430 Bezannes, France; bastien.bouchet@cryotera.fr
[3] French Society of Whole Body Cryotherapy (SFCCE), 75012 Paris, France
* Correspondence: guillaume.polidori@univ-reims.fr

Abstract: This study aims to investigate the impact of body heat loss on the thermal and aerodynamic conditions in a whole-body cryotherapy chamber. The underlying hypothesis is that the heat generated by the human body alters the thermal and aerodynamic environment inside the cabin. A numerical study was conducted to test this hypothesis and analyze the thermodynamic exchanges between the human body and the cabin during a 3 min whole-body cryotherapy session. The computational fluid dynamics (CFD) approach was used to study the unsteady heat transfer between the human body and the interior of the cryotherapy cabin. A thermal boundary condition, based on a mathematical model developed from experimental data, was applied to simulate skin cooling kinetics over time. The post-processing of the 3D results, including temperature, velocity fields, and thermal flux maps at the body surface, provided insight into the thermo-convective mechanisms involved in a whole-body cryotherapy session. The study found that body heat loss significantly affects the temperature fields inside the cabin, leading to global modifications of the aeraulic and thermal conditions. These findings suggest that cryotherapy protocols may need to be adjusted or the cabin set temperature optimized to enhance the therapeutic benefits.

Keywords: computational fluid dynamics (CFD); whole-body cryotherapy (WBC); skin temperature; extreme cold; human body

Citation: Elfahem, R.; Bouchet, B.; Abbes, B.; Polidori, G.; Beaumont, F. Influence of Body Heat Loss on Temperature and Velocity Fields in a Whole-Body Cryotherapy Chamber. *Fluids* **2023**, *8*, 252. https://doi.org/10.3390/fluids8090252

Academic Editors: Nilanjan Chakraborty and D. Andrew S. Rees

Received: 11 May 2023
Revised: 25 August 2023
Accepted: 14 September 2023
Published: 16 September 2023

1. Introduction

Whole-body cryotherapy (WBC) is a method that involves exposing one or more subjects to extremely cold dry air for a period of one to four minutes [1]. Studies have shown that cryotherapy provides physiological, psychological, and physical benefits [2–4]. Cryotherapy methods have been developed to improve recovery from exercise, and relieve pain, depression, and anxiety symptoms in patients with rheumatism and inflammatory diseases [5–7]. In order to achieve analgesic and anti-inflammatory effects, the patient undergoes a process of thermal shock, which involves the sudden and intense exposure of the body to extremely cold temperatures. This exposure induces a rapid decrease in skin temperature [8–10], triggering the desired therapeutic effects. The intensity of the thermal shock experienced during cryotherapy depends on the temperature and duration of exposure to extreme cold. Lower temperatures and longer durations of exposure lead to a more intense thermal shock, enhancing the physiological responses and potential therapeutic benefits [11].

The intensity of the thermal shock will therefore depend on the temperature difference between the inside of the cryotherapy chamber (from −110 to −195 °C, depending on the manufacturer) and the patient's skin temperature [12,13]. When discussing thermal shock, it is necessary to consider the aerodynamic aspect. The basic principle of cryotherapy is that exposure to cold activates thermosensitive skin receptors, which is believed to be the main

cause of the effectiveness of cryostimulation as it triggers regulatory mechanisms aimed at maintaining a constant core temperature. The resulting changes in skin temperature then become the key parameter on which the cryostimulation process relies. The thermal and metabolic response as it appears after cryostimulation is at least partially linked to what happened during the cryostimulation session, especially the speed of skin cooling.

The physiological response to extreme cold exposure is inherently linked to the thermal and airflow conditions within the cryotherapy chamber [14,15]. To achieve the expected therapeutic and analgesic effects, the temperature gradient between the human body and its environment must be significant [16]. Therefore, knowledge of the airflow and thermal conditions within the chamber throughout the cryotherapy session is fundamental [17]. Currently, there is a significant dearth of data in the scientific literature regarding the precise temperature conditions inside a whole-body cryotherapy cabin. This lack of available information underscores the need for further research and investigation in order to enhance our understanding of this specific aspect.

Furthermore, it is necessary to take into account all parameters that could affect the temperature within the chamber, especially the heat generated by the patient's body. Indeed, thermal transfers between the body and its environment can locally or on a larger scale modify temperatures inside the cryotherapy chamber. Depending on the size of the cryotherapy chamber, 1 to 3 patients can be accommodated, and it is difficult to precisely determine the impact of these heat sources on the actual temperature inside the chamber. It may be necessary to adjust the protocol duration or adjust the set temperature based on the number of patients present in the cryotherapy chamber. The first step in this reflection would be to estimate the impact of a single patient on the temperature inside a whole-body cryotherapy chamber. Currently, thermal measurements inside cryotherapy chambers are difficult due to the extreme temperatures that can damage the electronic circuits of measuring devices. Another alternative is to use numerical means such as CFD (Computational Fluid Dynamics), which allows for a precise approach to the airflow and thermal conditions within a cryotherapy chamber. CFD also provides access to flow variables that are difficult to obtain experimentally under extreme conditions. In a recent study, we used CFD to perform thermodynamic modeling aimed at optimizing the circulation of cold air flows in a partial-body cryotherapy chamber using an electric cooling system that produces air at −30 °C [18]. The numerical results were compared to experimental results, which demonstrated the potential of the method we developed.

In this study, we model the thermodynamic transfers between the human body and its environment during a 3 min whole-body cryotherapy session. The ultimate goal is to determine the influence of the heat input from the human body on the temperature fields inside the cryotherapy chamber. To assess the influence of heat transfer between the human body and its environment, a comparison of thermal conditions was conducted between the empty cryotherapy cabin and the cryotherapy cabin with a patient inside. A CFD calculation code based on the finite volume method was used to study the unsteady evolution of heat transfers. The results, presented in the form of temperature fields, velocity, and thermal flux maps on the body surface, provide a better understanding of the thermo-convective mechanisms involved during a whole-body cryotherapy session. This study is the first step in the process of adapting cryotherapy protocol duration and/or cryotherapy chamber set temperature according to the number of patients inside the chamber.

2. Materials and Methods

2.1. Geometry and Computational Domain

This section describes the first step of the numerical process used in the study, which involves defining the geometry of the whole-body cryotherapy (WBC) cabin and the human body inside it. The geometry of the cabin (see Figure 1) was created using computer-aided design (CAD) software ANSYS Workbench© Design Modeler (ANSYS 2020 R2, ANSYS, Inc., Canonsburg, PA, USA), based on the main dimensional characteristics of the cryotherapy cabin (interior dimensions: 2.1 m by 2.15 m, with a total height of 2.25 m). The geometry of

the human body was obtained using 3D scanning of a person wearing cryotherapy-specific protective clothing and was modeled as a heat transfer surface without considering the internal physical properties of the body. Figure 2 further demonstrates the application of the two planes, P1 and P2, employed in post-processing the results. These planes intersect the body within two mutually perpendicular median planes. The simulations focus on air circulation and heat transfer between the human body and its environment, without taking into account the complex biological mechanisms of the human body. The resulting numerical model allows for the analysis of the thermo-convective mechanisms involved in a WBC session and provides a better understanding of the impact of the heat generated by the human body on the temperature fields inside the cryotherapy cabin.

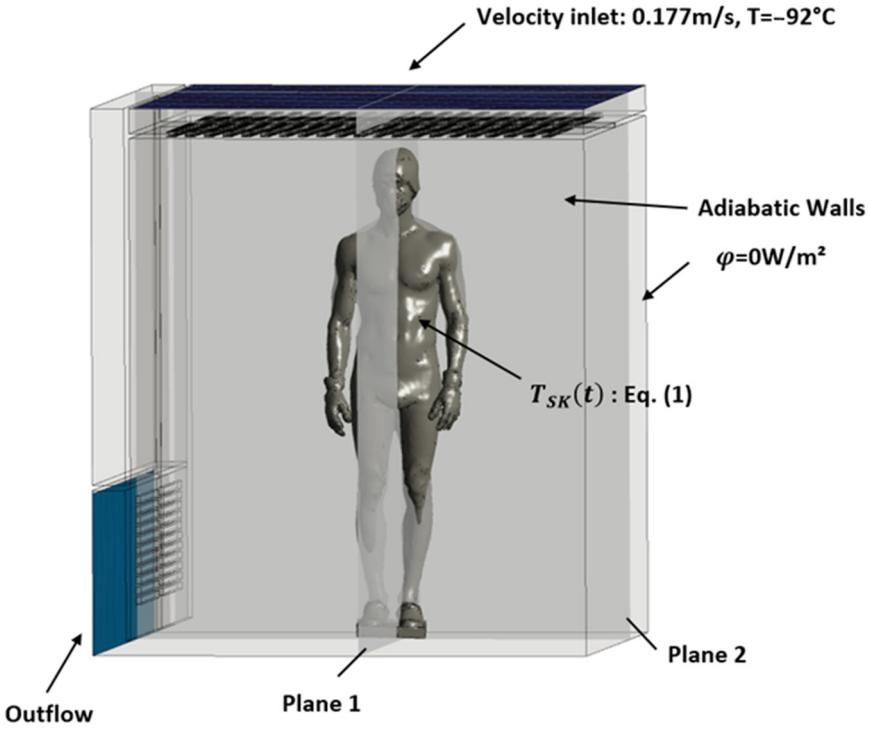

Figure 1. Boundary conditions.

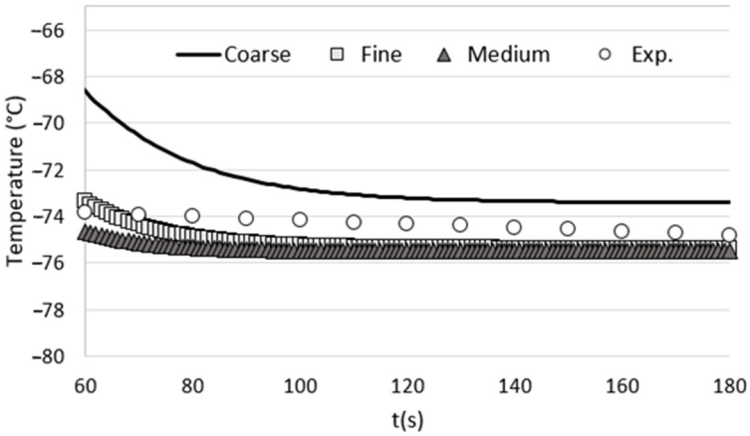

Figure 2. Comparison of the time evolution of the temperature at the center of the cryotherapy cabin for each tested grid with the temperatures measured experimentally.

2.2. Boundary Conditions

The boundary conditions of the problem are presented in Figure 1. Cold air is injected at the ceiling of the WBC cabin at a temperature of −92 °C and a constant velocity of 0.177 m/s, which corresponds to the incoming air flow rate given by the manufacturer of

the equipment (Mecotec, Germany). An outflow condition is applied at the ventilation grilles located at the bottom of the chamber. For simplification, the walls of the chamber are considered adiabatic. To model the evolution of skin temperature during a whole-body cryotherapy session, a thermal boundary condition is applied to the surface of the body. Equation (1) describes the evolution of skin temperature during a WBC session. This mathematical model of skin cooling kinetics was developed based on experimental data [13]. If we assume an exponential behavior for the initial transient phase [16] within the time range $t \in [0;30]$, and then switch to a linear trend during the latter part of the transient phase from $t \in [30;\beta]$, we can represent the time-varying skin temperature as follows:

$$T_{SK}(t) = \left[Ke^{-(at)^n}\right]_{0\to 30} + [At + B]_{30\to\beta} \quad (1)$$

where K, a, A, and B are constants to be analytically determined using both thermal boundary conditions and a C^1-continuous junction between these two functions.

The resulting analytical expression of the skin temperature is

$$T_{SK}(t) = \left[T_{sk0}\left(\frac{T_{sk0}}{Tsk_1 + C_0(30-\beta)}\right)^{-\left(\frac{t}{30}\right)^n}\right]_{0\to 30} + [C_0 t + (T_{sk1} - C_0\beta)]_{30\to\beta} \quad (2)$$

$$\text{with } n = \left(\frac{-30C_0}{[T_{sk1} + C_0(30-\beta)]ln\left(\frac{T_{sk0}}{Tsk_1 + C_0(30-\beta)}\right)}\right) \quad (3)$$

Tsk_0, Tsk_1, and C_0 are, respectively, the baseline skin temperature, the skin temperature at the end of the session, and the rate of cooling, and β corresponds to the end of the session.

In this calculation, the system was initialized at a temperature of −76 °C, which corresponds to the average temperature measured experimentally in the cryotherapy chamber. To account for the evolution of the thermo-physical properties of air with temperature, polynomial laws were implemented in the computational code. They allow for the calculation of the density, dynamic viscosity, thermal conductivity, and specific heat at each time step within the temperature range of interest (−110 °C to 33 °C).

The iterative calculation was performed over a duration of 3 min with a time step of 0.02 s. We chose two different planes to analyze the kinetics of temperature and velocity evolution and to study the dissipation of heat from the human body into the ambient air. The two planes that intersect the body along its symmetry axes are shown in Figure 1.

2.3. Computational Grid

To assess the influence of mesh size on the accuracy of our numerical results, we conducted a grid-dependency test. This involved performing calculations using three different grid configurations: coarse, medium, and fine. The number of cells for each grid and the corresponding computation time are provided in Table 1.

Table 1. Number of cells in each tested grid and associated computation time.

Grid	Mesh Nodes	Computational Cost (Hours)
Coarse	7.68×10^5	6
Medium	1.42×10^6	14
Fine	2.56×10^6	28

In order to evaluate the influence of grid size on the computational results, we conducted unsteady calculations on a reference case involving an empty cryotherapy cabin. The boundary conditions used in the grid-dependency test were strictly consistent with those described in the article. To assess the impact of grid size, we monitored the temperature at the center of the cabin, specifically at a height of 1 m from the cabin floor. Subsequently, we compared these numerical results with the experimental measurements

obtained from an empty cryotherapy cabin (without any patients inside). The comparison between the numerical results obtained for each tested grid and the experimental measurements is presented in Figure 2. The results show that the medium mesh gives results that are close to those obtained with the fine mesh, but with a calculation time that is twice as short. For optimal accuracy and computation time, we have chosen the parameters of the medium grid to perform the various grids of this study.

The meshing procedure involves generating a surface mesh on the body and subsequently creating a Cartesian volume mesh in the fluid domain. Regarding the dimensional criteria of the average mesh, all mesh elements within the calculation domain are smaller than or equal to 0.023 m. The cell size applied to the body ensures good resolution of the boundary layer and sufficient accuracy for thermal transfer and convection calculations in the air. The structured Cartesian mesh improves the convergence of results and limits the number of mesh cells. In total, the mesh of the computational domain including the human's body consists of over 3.5 million cells. Figure 3 showcases the mesh structure encompassing the body walls and its surroundings within the computational domain.

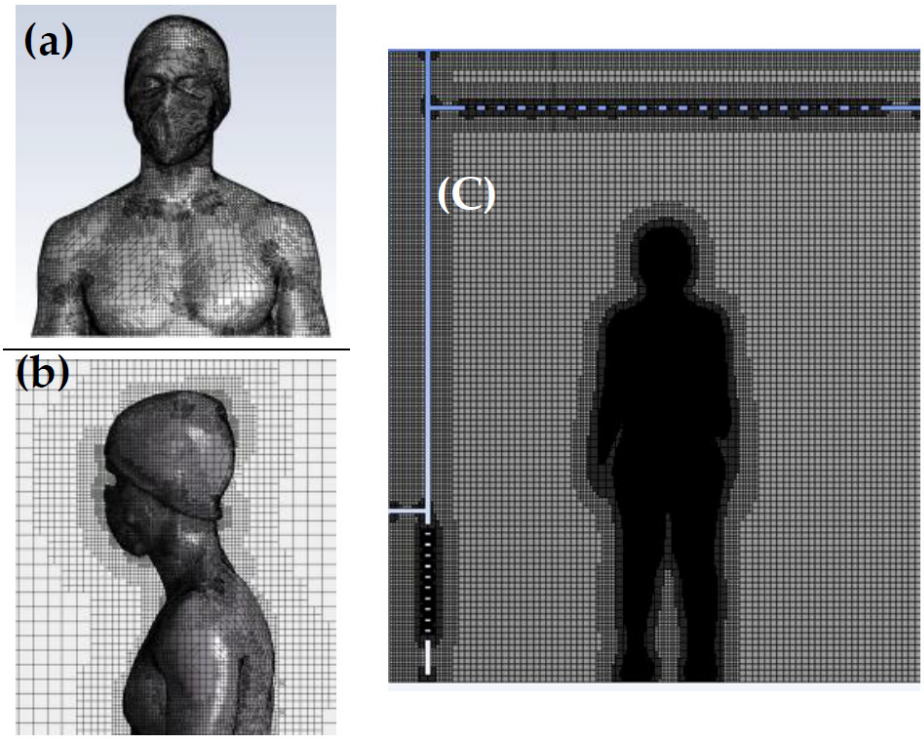

Figure 3. (**a**) Surface mesh on the body; (**b**) detailed view of the inflation mesh around the body displayed in a 2D vertical plane intersecting the body. (**c**) Overview of the computational domain.

2.4. Numerical Methods

In this study, we used the commercial calculation code ANSYS Fluent® 2020 R2. This CFD calculation code based on the finite volume method allows the solution of the system of equations governing fluid flow. The numerical study is three-dimensional, time-dependent, and non-isothermal. The SIMPLE algorithm was preferred to solve the pressure-velocity coupling, using a first-order discretization scheme [18]. The standard k-ε turbulence model was chosen for closure of the Reynolds-averaged Navier–Stokes equations. Heat transfer as well as mass transfer by convection are described by the following equations:

Mass conservation equation:

$$\frac{\partial \rho}{\partial t} + \nabla \cdot (\rho v) = 0 \quad (4)$$

Momentum conservation equation:

$$\frac{\partial(\rho v)}{\partial t} + \nabla\cdot(\rho v \otimes v) = -\nabla p + \nabla \cdot \tau \tag{5}$$

Energy conservation equation (heat transfer):

$$\frac{\partial(\rho e)}{\partial t} + \nabla\cdot(\rho e v) = -p\nabla\cdot v + \nabla\cdot(q + q_{turb}) \tag{6}$$

where p is the pressure, ρ is the fluid density, t is the time, v is the fluid velocity vector, p is the pressure, τ is the viscous stress tensor, e is the specific internal energy, q is the conductive heat flux vector, and q_{turb} represents the turbulent heat flux vector.

3. Results

Figure 4 displays the distribution of air flow velocities (a) and temperatures (b) for plane P1 at t = 1, 2, and 3 min, respectively, while Figure 5 illustrates the distribution of air flow velocities (a) and temperatures (b) for plane P2 at t = 1, 2, and 3 min, respectively. Note that we have limited the temperature range to between −92 °C and −72 °C and the velocity range to between 0 and 1.5 m/s to highlight even small gradients of velocity or temperature.

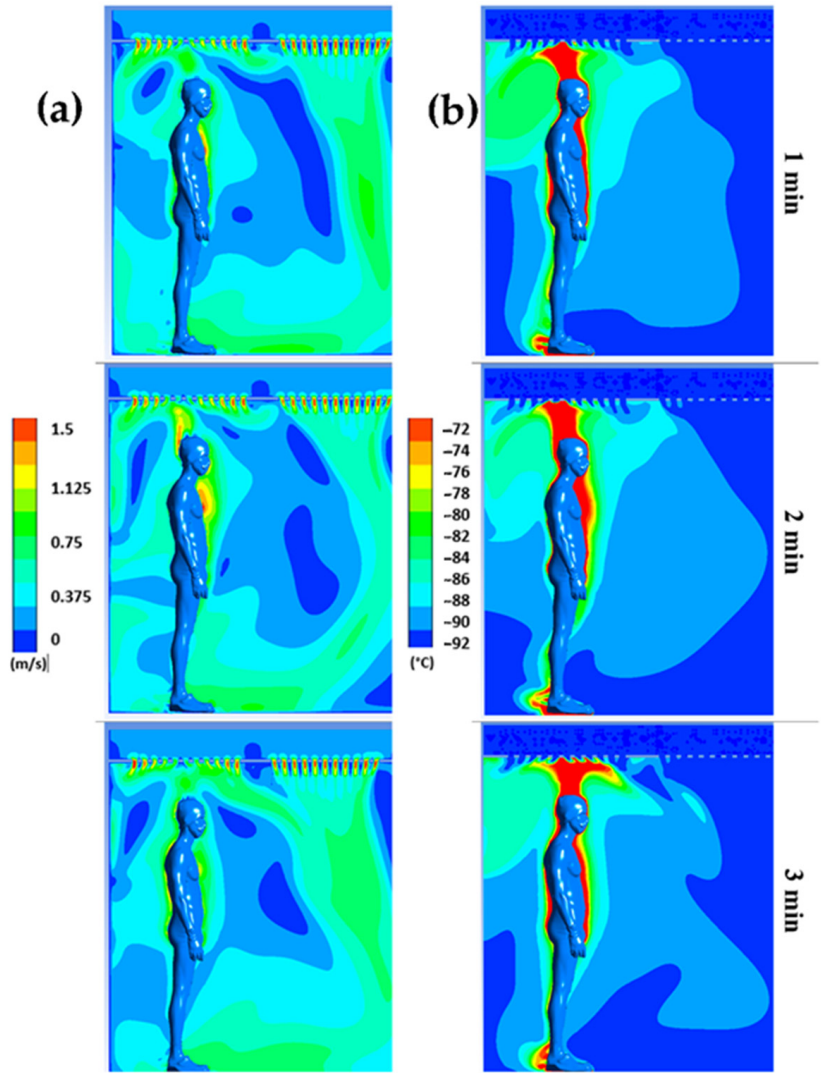

Figure 4. Velocity (**a**) and temperature (**b**) fields for plane P1 at t = 1 min, t = 2 min, and t = 3 min.

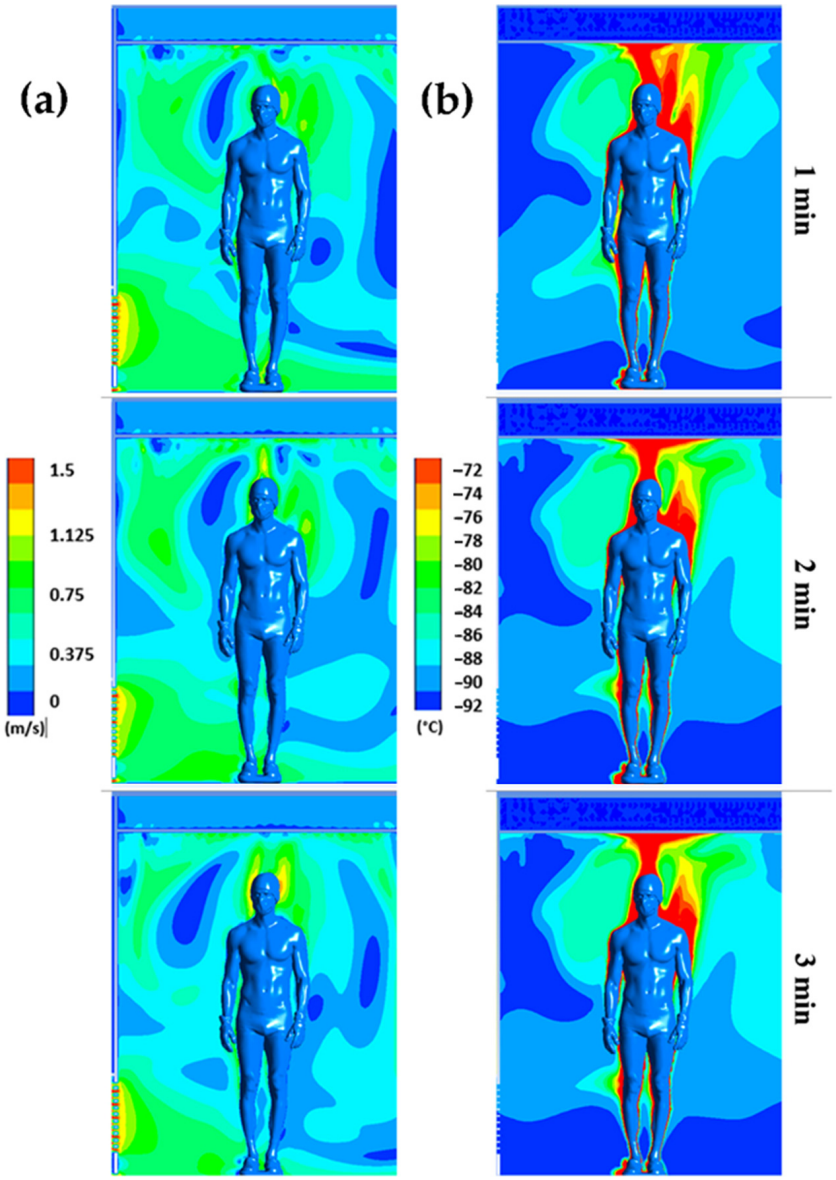

Figure 5. Velocity (**a**) and temperature (**b**) fields for plane P2 at t = 1 min, t = 2 min, and t = 3 min.

The results confirm a strong heterogeneity of temperatures in the chamber, with one of the main reasons being the presence of the human body, which behaves both as an obstacle and as a source of heat. The results also indicate that the highest temperatures are located near the body, while the coldest temperatures are located in the areas far from the body.

We can observe that the highest velocities are located around the body and above the head, due to the development of a thermal plume around the body. This thermal plume, which accelerates the airflow in the boundary layer and the heat transfers within the chamber, has a maximum velocity estimated at 1.3 m/s. To complement the results, Figure 4 illustrates the trajectory of the streamline in the WBC chamber at t = 60 s.

The streamlines are colored by the vertical velocity, with a range limited to the interval of −0.5 to 0.5 m/s to better illustrate the smallest gradient of velocity. The streamlines allow us to highlight the three-dimensional structure of the flow in the cryotherapy chamber at t = 60 s. The 3D streamlines (Figure 6a) show that the flow is composed of multiple vortex structures that interact with each other. The streamlines represented in a plane (Figure 6b) indicate that the human body acts as an obstacle for the flow of air coming from the ceiling of the chamber. The presence of large vortex structures indicates an interaction between the upward flows in the vicinity of the body and the downward flows resulting from the

injection of cold air into the chamber. The air warmed by contact with the body, with a lower density, tends to rise, while the cold air, with a higher density, descends to the floor.

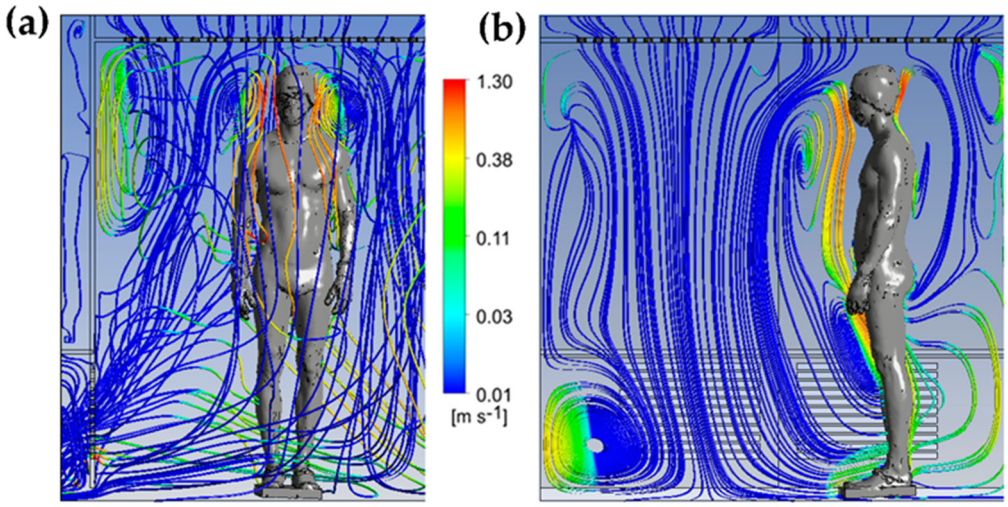

Figure 6. Streamlines colored by the vertical velocity component at t = 60 s in 3D (**a**); 2D streamlines plotted in a vertical plane passing through the body and colored by the vertical velocity component (**b**).

To complete, Figure 7 shows the distribution of surface flux on the human body at t = 180 s. Note that the range has been limited to the interval of 200 to 2000 W/m^2 to better visualize the differences.

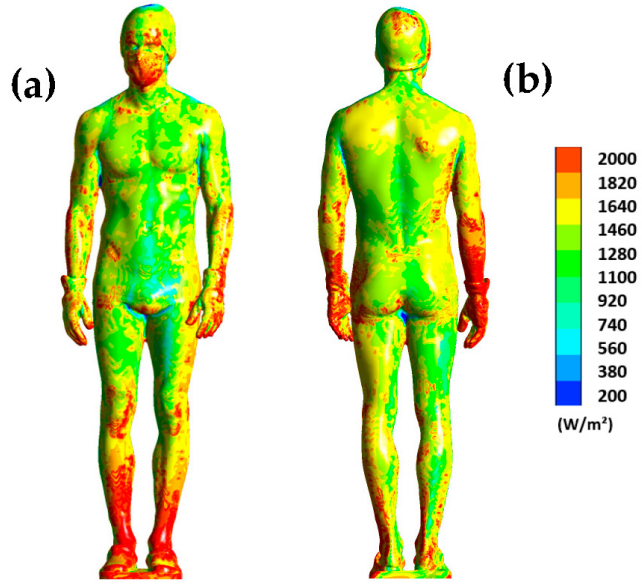

Figure 7. Surface heat flux dissipated by the human body at t = 180 s for the front side (**a**) and the back side (**b**).

The results show us that the distribution of heat flux on the body is uneven. For example, the legs dissipate much more heat, especially at the ankles where the dissipated flux exceeds 2000 W/m^2. The same observation can be made for the back of the wrists. This Figure highlights the areas that are more likely to cool down, such as the legs or forearms, because a high heat flux indicates significant heat dissipation. Note also that the distribution of heat flux on the surface of the human body is inherently dependent on the aerodynamic conditions inside the chamber. Thus, the higher the air velocity, the more heat is dissipated.

To emphasize the impact of body heat on the overall temperature during a cryotherapy session, we conducted temperature monitoring at multiple points within the empty cabin and the cabin with a human body. Figure 8 presents a histogram comparing the average temperatures recorded at three different heights (0.48 m, 1.02 m, and 1.84 m) in both setups. The measurements were taken at five positions, with four located 15 cm away from the walls and one at the middle of the cabin (Figure 8b).

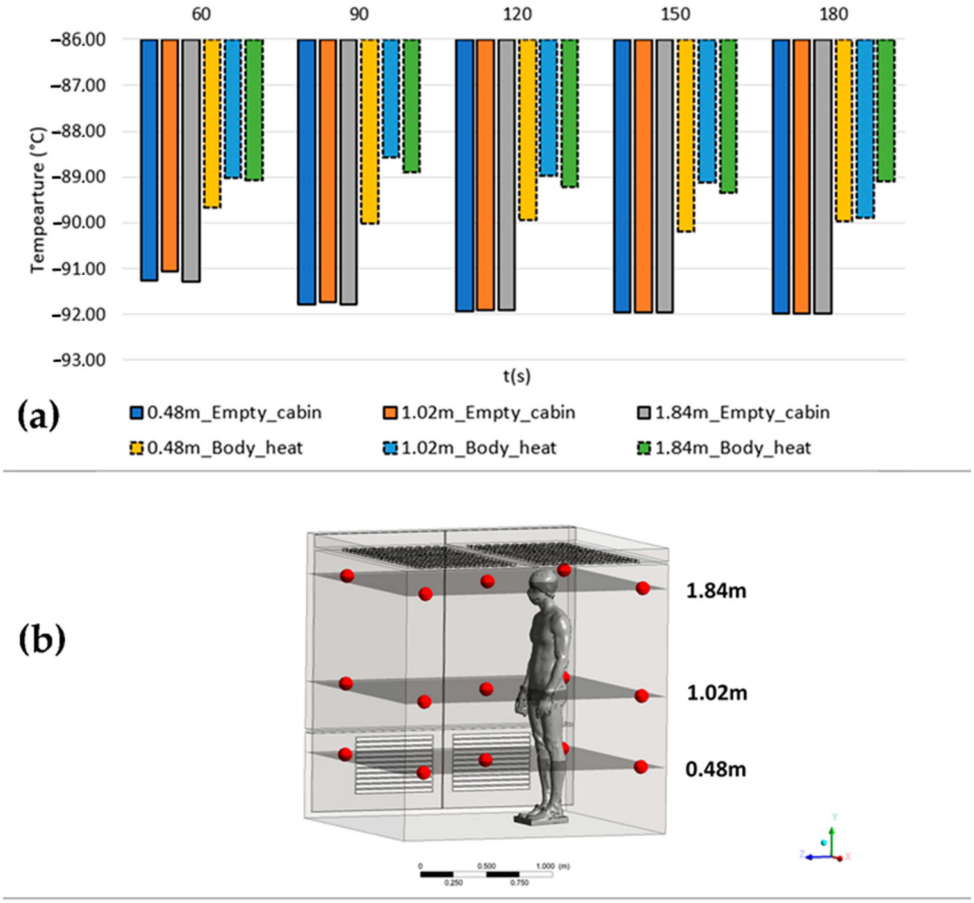

Figure 8. Average temperatures recorded at three different heights (0.48 m, 1.02 m, and 1.84 m) in the empty cabin and the cabin with a human body (**a**); location of the measurement points within the cabin (**b**).

The obtained results reveal two significant observations. Firstly, in the absence of a patient, the temperatures in the empty cabin tend to decrease within the initial 120 s. However, when a patient is present, the temperatures exhibit fluctuations over time. Secondly, there are temperature variations ranging from 1 to 3 degrees Celsius between the measured temperatures in the empty cabin and those estimated when accounting for the human body's heat input.

Moreover, the temperatures recorded at different heights in the empty cabin exhibit relatively uniform values with minor deviations. In contrast, when a patient is present in the cabin, noticeable deviations occur, which vary in significance depending on both the height and the duration of the cryotherapy session.

4. Discussion

The results confirm the hypothesis that the heat input from the human body significantly increases the temperatures within the WBC chamber, as the human body transfers heat to the nearby environment [19]. During exposure to cold, the layer of air, i.e., the boundary layer, developing at the surface of the human body limits the transfer of heat

from the body to the air inside the chamber [20]. The development of this boundary layer is visible in Figures 3 and 4 in the form of a thermal plume that rises upward and induces thermal stratification in the chamber. Several articles in the literature have highlighted the formation of a thermal plume during WBC sessions [21] or PBC (Partial Body Cryotherapy) sessions [18,22].

Heat exchange between the human body and its environment in indoor spaces has also been the subject of scientific studies [23]. A study conducted by Settles and Craven [24] examined the development of the thermal plume created by the presence of an individual in an indoor environment. The researchers studied the interaction between a standing (clothed) man and his environment (a closed and unventilated room at ambient temperature). The experimental and numerical results revealed that the flow velocity could reach 0.24 m/s above the subject's head [24]. The difference in temperature gradient between the skin temperature of the human body (around 33 °C on average) and the air temperature in the cryotherapy chamber (−90 to −110 °C) is considerably greater in our study.

Therefore, the convection flow velocity is naturally higher. The results obtained in our study are consistent with those of Marreiro et al. [21] who estimated the velocity of the thermal plume dissipating above a subject during a whole-body cryotherapy session at −110 °C. In their study, the velocity measured in the thermal plume was about 1.5 m/s [21], while it is estimated to be around 1.3 m/s in the present study.

Concretely, the thermal plume that develops around the body accelerates the air flow in the boundary layer as well as the heat transfer within the chamber. These results confirm the hypothesis that the heat generated by the human body modifies the aerodynamic and thermal conditions within the chamber. This results in an overall increase in temperature within the chamber, which leads to a decrease in the value of the surface flux that is particularly notable for certain parts of the body such as the abdomen (Figure 7). The distribution of the thermal flux suggests a more pronounced cooling in the lower part of the body, where the thermal plume develops. Moreover, the air flow tends to accelerate the heat transfer between the human body and its environment through a forced convection phenomenon [17]. Burkov et al. [25] demonstrated that the dissipated surface heat flux for a person of normal weight was 1775 W/m^2 after a 3 min exposure to −178 °C in a partial-body cryotherapy chamber. In our study, the thermal flux was 1227.10 W/m^2 for an exposure temperature of −92 °C. The discrepancies observed between their study and ours are likely attributed to the difference in exposure temperature, as the lower the temperature, the greater the dissipation of surface heat flux. It is worth noting that, during the 3 min cryotherapy session, the surface heat flux decreases by approximately 10%. However, Yerezhep et al. [26] estimated that, during a partial-body cryotherapy session, the thermal flux decreases by about one-third. It should be emphasized that the value of the flux is inherently dependent on the air temperature within the cryotherapy chamber and the prevailing airflow conditions.

On the one hand, the resulting flow displaces warm air around the body, but on the other hand, it accelerates the heat transfer between the human body and the air inside the cryotherapy chamber. This leads to a progressive increase in temperatures within the treatment space (Figures 4 and 5), which in turn will modify the distribution of heat flux at the surface of the human body. What is also interesting is that the flows associated with the thermal plume are counter-current to the flows of air injected to cool the cryotherapy chamber. This process will generate a series of vortical structures allowing a mixing of the flow within the chamber while limiting the phenomena of thermal stratification that could occur if there were no heat source.

Finally, the comparison of temperatures between an empty cabin and the cabin with a patient serves to confirm the significant impact of the human body's heat input on the overall temperature within the cabin. Our results demonstrate that the heat generated by the human body is capable of significantly increasing the temperature of its immediate surroundings, even under extreme conditions such as cryotherapy.

Given that multiple patients can participate in a cryotherapy session simultaneously, further studies are needed to evaluate the impact of these heat sources on the temperature inside the cryotherapy chamber. Indeed, a significant increase in temperature within the chamber could reduce the therapeutic effectiveness of cryotherapy.

Limitations

The results of this study need to be interpreted in light of several limitations. First, the numerical model does not take into account the physiological behavior of the human body. Indeed, the interaction between the human body and the cabin occurs mainly at the skin level, and the skin temperature can reflect the balance between heat loss to the environment and heat produced by metabolically active tissues. Furthermore, the thermal boundary condition imposed on the human body assumes that at time t = 0, the surface temperature is uniformly distributed over the body surface, whereas, in reality the thermal response differs depending on the body segment. Finally, the patient is static, while in reality, patients are asked to move, which generates disturbances in the flow field and local modification of heat transfers.

5. Conclusions

The objective of this study was to investigate the impact of the heat generated by the human body on the thermal and aerodynamic conditions inside a whole-body cryotherapy chamber (WBC). To achieve this, a 3 min cryotherapy session was modeled using a computational fluid dynamics (CFD) method. To assess the influence of heat transfer between the human body and its environment, a comparison of thermal conditions was conducted between the empty cryotherapy cabin and the cryotherapy cabin with a patient inside. A thermal boundary condition was applied to the body based on a mathematical model developed from experimental data, enabling simulation of the skin cooling kinetics over time.

The major findings are:

- The presence of multiple vortical cells continuously modify thermal and aerodynamic conditions inside the chamber;
- The human body's thermal plume interacts with cold air from the ceiling, resulting in counter-rotating vortical cells;
- A close relationship between temperature distribution on the body surface and unsteady flow dynamics within the chamber;
- The significant impact of the human body's heat input on overall temperature in the cabin.

Further experimental measurements and calculations are required to quantify the impact of one or more patients on the temperature fields within a cryotherapy chamber. These preliminary results also suggest the need to adapt cryotherapy protocols or adjust the set temperature to account for the heat input from the human body.

Author Contributions: Conceptualization, R.E. and G.P.; methodology, F.B.; software, R.E.; validation, B.A., G.P. and B.B.; formal analysis, F.B.; investigation, G.P.; resources, B.B.; data curation, B.A.; writing—original draft preparation, F.B.; writing—review and editing, R.E.; visualization, G.P.; supervision, B.A.; project administration, B.B. All authors have read and agreed to the published version of the manuscript.

Funding: This research received no external funding.

Data Availability Statement: The datasets generated during the current study are available from the first author on reasonable request.

Conflicts of Interest: The authors declare no conflict of interest.

References

1. Polidori, G.; Taiar, R.; Legrand, F.; Beaumont, F.; Murer, S.; Bogard, F.; Boyer, F.C. Infrared thermography for assessing skin temperature differences between Partial Body Cryotherapy and Whole Body Cryotherapy devices at −140 °C. *Infrared Phys. Technol.* **2018**, *93*, 158–161. [CrossRef]
2. Hausswirth, C.; Schaal, K.; Le Meur, Y.; Bieuzen, F.; Filliard, J.-R.; Volondat, M.; Louis, J. Parasympathetic activity and blood catecholamine responses following a single partial-body cryostimulation and a whole-body cryostimulation. *PLoS ONE* **2013**, *8*, e72658. [CrossRef]
3. Banfi, G.; Melegati, G.; Barassi, A.; Dogliotti, G.; Melzi d'Eril, G.; Dugué, B.; Corsi, M.M. Effects of whole-body cryo-therapy on serum mediators of inflammation and serum muscle enzymes in athletes. *J. Therm. Biol.* **2009**, *34*, 55–59. [CrossRef]
4. Straburzyńska-Lupa, A.; Kasprzak, M.P.; Romanowski, M.W.; Kwaśniewska, A.; Romanowski, W.; Iskra, M.; Rutkowski, R. The Effect of Whole-Body Cryotherapy at Different Temperatures on Proinflammatory Cytokines, Ox-idative Stress Parameters, and Disease Activity in Patients with Ankylosing Spondylitis. *Oxid. Med. Cell Longev.* **2018**, *2018*, 2157496. [CrossRef] [PubMed]
5. Algafly, A.A.; George, K.P. The effect of cryotherapy on nerve conduction velocity, pain threshold and pain tolerance. *Br. J. Sports Med.* **2007**, *41*, 365–369. [CrossRef] [PubMed]
6. Rymaszewska, J.; Ramsey, D.; Chładzińska-Kiejna, S. Whole-body cryotherapy as adjunct treatment of depressive and anxiety disorders. *Arch. Immunol. Ther. Exp.* **2008**, *56*, 63–68. [CrossRef]
7. Vitenet, M.; Tubez, F.; Marreiro, A.; Polidori, G.; Taiar, R.; Legrand, F.; Boyer, F.C. Effect of whole body cryotherapy interventions on health-related quality of life in fibromyalgia patients: A randomized controlled trial. *Complement. Ther. Med.* **2018**, *36*, 6–8. [CrossRef]
8. Cholewka, A.; Stanek, A.; Sieroń, A.; Drzazga, Z. Thermography study of skin response due to whole-body cryotherapy. *Skin Res. Technol.* **2012**, *18*, 180–187. [CrossRef]
9. Fonda, B.; De Nardi, M.; Sarabon, N. Effects of whole-body cryotherapy duration on thermal and cardio-vascular response. *J. Therm. Biol.* **2014**, *42*, 52–55. [CrossRef]
10. Costello, J.T.; McInerney, C.D.; Bleakley, C.M.; Selfe, J.; Donnelly, A.E. The use of thermal imaging in assessing skin temperature following cryotherapy: A review. *J. Therm. Biol.* **2012**, *37*, 103–110. [CrossRef]
11. Bleakley, C.; Bieuzen, F.; Davison, G.W.; Costello, J.T. Whole-body cryotherapy: Empirical evidence and theoretical perspectives. *Open Access J. Sports Med.* **2014**, *5*, 25–36. [CrossRef]
12. Bleakley, C.; Hopkins, J. Is it possible to achieve optimal levels of tissue cooling in cryotherapy? *Phys. Ther. Rev.* **2010**, *15*, 344–350. [CrossRef]
13. Polidori, G.; Elfahem, R.; Abbes, B.; Bogard, F.; Legrand, F.; Bouchet, B.; Beaumont, F. Preliminary study on the effect of sex on skin cooling response during whole body cryostimulation (−110 °C): Modeling and prediction of exposure durations. *Cryobiology* **2020**, *97*, 12–19. [CrossRef]
14. Stocks, J.M.; Taylor, N.A.S.; Tipton, M.J.; Greenleaf, J.E. Human physiological responses to cold exposure. *Aviat. Space Environ. Med.* **2004**, *75*, 444–457. [PubMed]
15. Castellani, J.W.; Young, A.J. Human physiological responses to cold exposure: Acute responses and acclimatization to prolonged exposure. *Auton. Neurosci. Thermoregul.* **2016**, *196*, 63–74. [CrossRef] [PubMed]
16. Huizenga, C.; Zhang, H.; Arens, E.; Wang, D. Skin and core temperature response to partial-and whole-body heating and cooling. *J. Therm. Biol.* **2004**, *29*, 549–558. [CrossRef]
17. Bouzigon, R.; Arfaoui, A.; Grappe, F.; Ravier, G.; Jarlot, B.; Dugue, B. Validation of a new whole-body cryotherapy chamber based on forced convection. *J. Therm. Biol.* **2017**, *65*, 138–144. [CrossRef] [PubMed]
18. Beaumont, F.; Bogard, F.; Hakim, H.; Murer, S.; Bouchet, B.; Polidori, G. Modeling of an Innovative Nitrogen-Free Cryotherapy Device. *Dynamics* **2021**, *1*, 204–216. [CrossRef]
19. Savic, M.; Fonda, B.; Sarabon, N. Actual temperature during and thermal response after whole-body cryotherapy in cryo-cabin. *J. Therm. Biol.* **2013**, *38*, 186–191. [CrossRef]
20. Schlichting, H.; Gersten, K. *Boundary-Layer Theory*; Springer: Berlin/Heidelberg, Germany, 2016.
21. Marreiro, A.; Beaumont, F.; Taiar, R.; Polidori. Application des techniques d'imagerie thermique infrarouge et de mécanique des fluides numérique à la cryothérapie corps entier (CCE). *Instrum. Mes. Métrologie* **2017**, *6*, 11–32.
22. Beaumont, F.; Bogard, F.; Murer, S.; Anger, D.; Bouchet, B.; Polidori, G. Partial body cryotherapy in confined cryosaunas: Effects of inherent thermal stratification. *Ser. Biomech.* **2018**, *32*, 12–17.
23. Liu, Y.; Liu, Z.; Luo, J. Numerical Investigation of the Unsteady Thermal Plume around Human Body in Closed Space. *Procedia Eng.* **2015**, *131*, 1919–1926. [CrossRef]
24. Craven, B.A.; Settles, G.S. A computational and experimental investigation of the human thermal plume. *ASME. J. Fluids Eng.* **2006**, *128*, 1251–1258. [CrossRef]
25. Burkov, A.; Kolishkin, L.M.; Pushkarev, A.V.; Shakurov, A.V.; Tsiganov, D.I.; Zherdev, A.A. Experimental and computational thermal analysis of partial-body cryotherapy. *Int. J. Heat Mass Transf.* **2022**, *183*, 122194. [CrossRef]
26. Yerezhep, D.; Yemelyanov, A.; Kuznetsov, Y.; Perminov, A.; Pronin, V.; Minikaev, A.; Yerezhep, A. Computer analysis of the thermal state of the object after cryotherapy. *J. Phys. Conf. Ser.* **2019**, *1333*, 032092. [CrossRef]